embedding staining of PAM-1 antibody internalized for 20 min at 37°C by PAM-1/TS/AA cells. Label was seen in immature SGs (arrows). Scale bar, 200 nm. (**B**) PAM-1 antibody was internalized for 20 min at 37°C by PAM-1/TS/AA cells, the cells were fixed and prepared for cryosectioning. PAM-1 antibody in the sections was detected with 10 nm protein A-gold (arrowheads). After blocking, the sections were then stained with ACTH antibody detected with 15 nm protein A-gold. Scale bar, 200 nm. Antibody internalized for 20 min at 37°C by PAM-1/TS/AA (**C**) and PAM-1/TS/DD (**D**) cells was visualized along with with chromogranin A. Scale bar, 10 µm. The figures represent thin optical sections not including the tips of the cell processes.

Figure 10: Mutations affecting PAM cytosolic domain phosphorylation affect fate of surface biotinylated PAM-1. (**A**) AtT-20 lines expressing PAM-1/TS/AA or TS/DD were analyzed using the biotinylation stability paradigm described in **Fig. 2A**; PAMs and PHMs secreted basally during the 1 h and 4 h chase periods were also quantified. (**B**) Data for the 1 h chase were quantified relative to biotinylated PAM-1. (**C**) The stimulated secretion biotinylation paradigm described in **Fig. 1C** was used to analyze PAM-1/TS/AA and TS/DD cells. (**D**) Secretion of biotinylated PAMs and PHMs during the 0-60 min chase and the subsequent 30 min Basal or Stimulated collection was quantified relative to intact, biotinylated PAM.

SUPPORTING INFORMATION

Supplemental Table 1: Quantification in cryosections of gold particles detecting PAM-1 antibody internalized for 1 h. Gold particles decorating organelles were counted; the relative area for each organelle was determined by point counting and results are expressed as number of gold particles per μm^2 occupied by that organelle. Labeling over mitochondria was used as an estimate of non-specific labeling, yielding the labeling index. Label over SGs was not determined as immature SGs were not reliably distinguished from vacuolar endosomes (see **Supplemental Figure 1**).

Supplemental Figure 1: Images representative of those quantified in **Supplemental Table 1**. Gold particles were seen at the cell membrane (**A**), in tubular structures in the peripheral part of the TGN (**A,B**) and in MVBs (**B**). Electron dense condensation typical of the central tubules of the TGN were seen in **A,B**. Electron lucent structures located near the TGN and probably representing immature SGs are labeled in **C-E**. Scale bar, 200 nm.

Supplemental movie 1: PAM-1 cells were labeled with WGA-Alexa Fluor 488 and PAM antibody on ice, the temperature was raised to 37°C for 10 min and confocal images were then recorded every 60 sec for 40 min. The pattern of WGA uptake is best seen in the cell at lower right, which does not express PAM.

Supplemental movie 2: PAM-1 cells were labeled with WGA-Alexa Fluor 488 and PAM antibody on ice,

incubated for 2 h at 20°C and then incubated at 37°C; confocal images were then recorded every 60 sec for 45 min. The initial shift in focus plane is due to the temperature shift.

Supplemental figure 2: Representative images from movies 1 and 2. (**A**) Live images recorded 43-49 min after warming the cells to 37°C from labeling on ice. At lower arrowhead an endosome detaches from the TGN, fuses with a peripheral endosome and then again makes brief contact with the TGN. At upper arrowhead a peripheral endosomal fusion. Two PAM containing endosomes at the bottom of the image (arrows) remain stable during the 6 min period. (**B**) Live images recorded 30-40 min after warming the cells from 20C to 37°C. Only partially overlapping trafficking of PAM and WGA converges to the TGN area. At arrowhead a PAM containing endosome remaining stable during the 10 min period. Scale bars, 10 μm.

REFERENCES

1. Pelletier G. Secretion and uptake of peroxidase by rat adenohypophyseal cells. J Ultrastruct Res 1973;43:445-459.
2. Farquhar MG. Recovery of surface membrane in anterior pituitary cells. J Cell Biol 1978;77:R35-R42.
3. Farquhar MG. Membrane recycling in secretory cells: pathway to the Golgi complex. Ciba Foundation Symposium 92, Pitman Books Ltd., London, 1982, pp 157-183.
4. Romagnoli P, Herzog V. Reinternalization of secretory proteins during membrane recycling in rat pancreatic acinar cells. Eur J Cell Biol 1987;44:167-175.
5. Patzak A, Winkler H. Exocytotic exposure and recycling of membrane antigens of chromaffin granules: ultrastructural evaluation after immunolabeling. J Cell Biol 1986;102:510-515.
6. Milgram SL, Mains RE, Eipper BA. COOH-terminal signals mediate the trafficking of a peptide processing enzyme in endocrine cells. J Cell Biol 1993;121:23-36.
7. Hurtley SM. Recycling of a secretory granule membrane protein after stimulated secretion. J Cell Sci 1993;106:649-656.
8. Solimena M, Dirkx R, Hermel J-M, Pleasic-Williams S, Shapiro JA, Caron L, Rabin DU. ICA 512, an autoantigen of type I diabetes, is an intrinsic membrane protein of neurosecretory granules. EMBO J 1996;15:2102-2114.
9. Wasmeier C, Burgos PV, Trudeau T, Davidson HW, Hutton JC. An extended tyrosine-targeting motif for endocytosis and recycling of the dense-core vesicle membrane protein phogrin. Traffic 2005;6:474-487.
10. Subramaniam M, Koedam JA, Wagner DD. Divergent fates of P- and E-selectins after their expression on the plasma membrane. Mol Biol Cell 1993;4:791-801.

Organelle	% of total gold particles attributed to membrane organelle	Gold particles/μm^2 organelle profile	Labeling index (labeling over mitochondria = 1)
Tubular or vacuolar endosomal structures	60.30±2.67	0.57±0.03	3.8
Tubular, Golgi associated	11.41±2.15	0.32±0.03	2.1
Multivesicular body	9.93±1.19	0.84±0.23	5.6
Lysosome	8.79±1.38	0.31±0.02	2.1
Cisternal part of TGN adjacent to the Golgi stack	1.77±0.08	0.12±0.06	0.8
Golgi stack	2.62±0.77	0.07±0.01	0.5
Mitochondria	5.32±0.24	0.15±0.01	1

Supplemental table 1

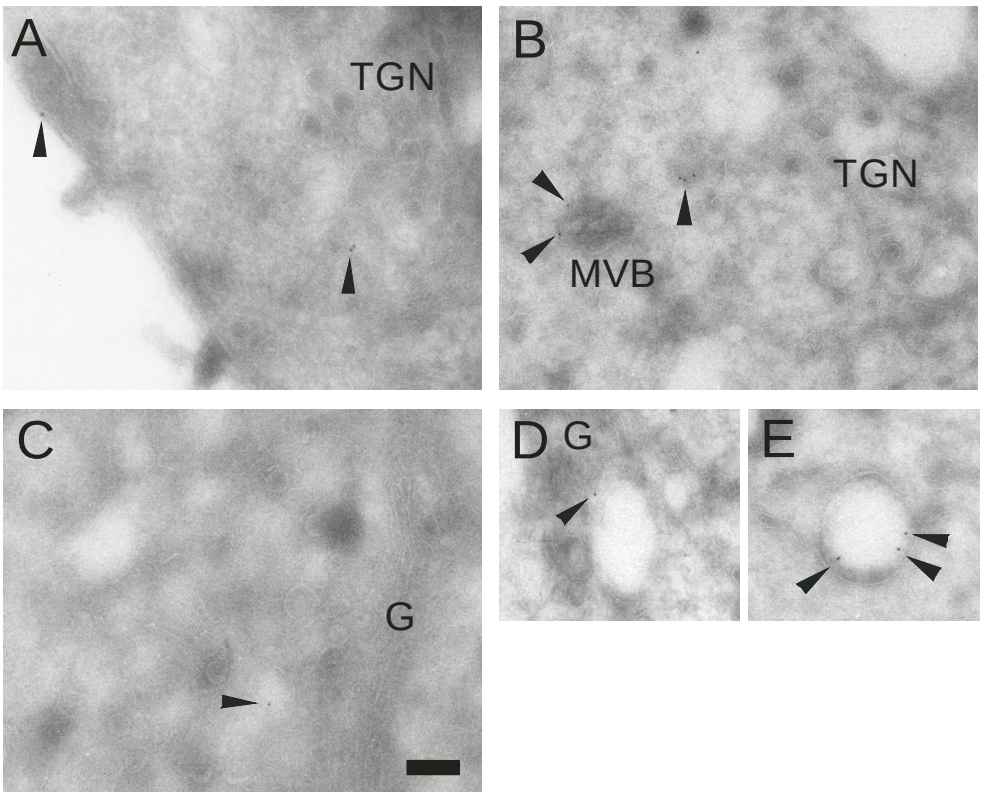

Supplemental Figure 1

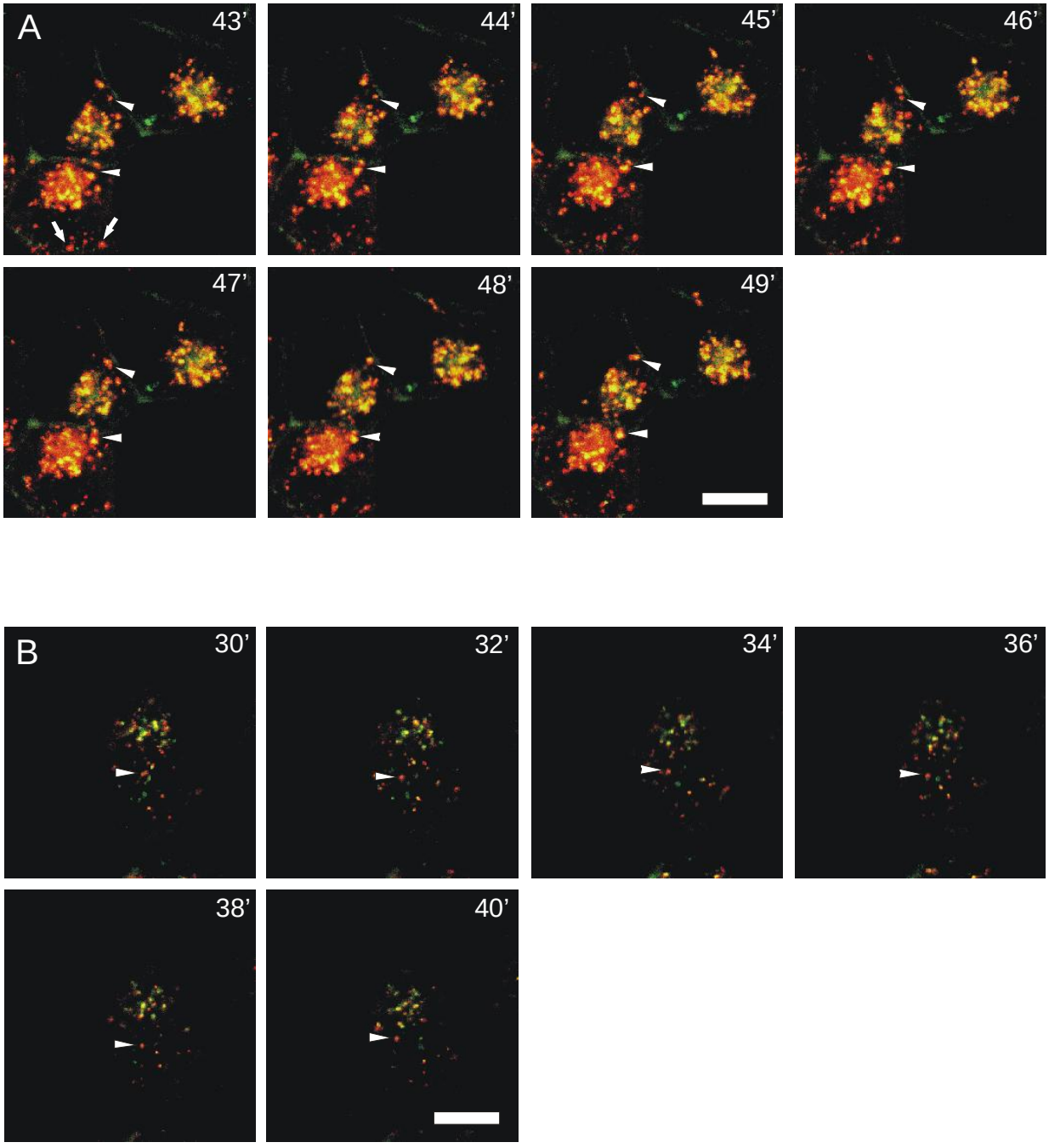

Supplemental Figure 2